Video Article

Generation of Heterogeneous Drug Gradients Across Cancer Populations on a Microfluidic Evolution Accelerator for Real-Time Observation

Ke-Chih Lin[1], Gonzalo Torga[2], Yusha Sun[1], Kenneth J. Pienta[2], James C. Sturm[1], Robert H. Austin[1]

[1]Princeton University

[2]Johns Hopkins Medical Institute

Correspondence to: Ke-Chih Lin at kechihl@princeton.edu

URL: https://www.jove.com/video/60185
DOI: doi:10.3791/60185

Keywords: Bioengineering, Issue 151, microfabrication, cancer-on-a-chip, tumor microenvironment, chemotherapy gradient, resistance, cell migration

Date Published: 9/19/2019

Citation: Lin, K.C., Torga, G., Sun, Y., Pienta, K.J., Sturm, J.C., Austin, R.H. Generation of Heterogeneous Drug Gradients Across Cancer Populations on a Microfluidic Evolution Accelerator for Real-Time Observation. *J. Vis. Exp.* (151), e60185, doi:10.3791/60185 (2019).

Abstract

Conventional cell culture remains the most frequently used preclinical model, despite its proven limited ability to predict clinical results in cancer. Microfluidic cancer-on-chip models have been proposed to bridge the gap between the oversimplified conventional 2D cultures and more complicated animal models, which have limited ability to produce reliable and reproducible quantitative results. Here, we present a microfluidic cancer-on-chip model that reproduces key components of a complex tumor microenvironment in a comprehensive manner, yet is simple enough to provide robust quantitative descriptions of cancer dynamics. This microfluidic cancer-on-chip model, the "Evolution Accelerator," breaks down a large population of cancer cells into an interconnected array of tumor microenvironments while generating a heterogeneous chemotherapeutic stress landscape. The progression and the evolutionary dynamics of cancer in response to drug gradient can be monitored for weeks in real time, and numerous downstream experiments can be performed complementary to the time-lapse images taken through the course of the experiments.

Video Link

The video component of this article can be found at https://www.jove.com/video/60185/

Introduction

Cancer has been increasingly recognized as a complex ecosystem that depends not only on the continued dysregulation of mutated cell populations but also on vital interactions between cancer cells and the host microenvironment. In this sense, cancer evolves on an adaptive landscape manifested by a combination of factors, including a heterogeneous tumor microenvironment and crosstalk with a variety of host cells, all of which contribute selective pressures for further genetic or epigenetic changes[1,2,3]. In the context of solid tumors, uneven distribution of chemotherapeutics and other resource gradients contributes to their molecular heterogeneity and may play a role in the development of drug resistance, increased angiogenesis to particular tumor subpopulations, and even metastasis[4,5,6]. Conventional in vitro 2D cell culture studies, while possessing large-scale, convenient experimental capacity, provides mean-field, uniform, and fixed conditions, often lacking the precise spatial and temporal environmental control necessary to truly emulate in vivo tumor dynamics. Thus, there is a need for more representative ex vivo models to reproduce the tumor microenvironment prior to animal models in the drug development pipeline in order for a better prediction of cancer progression as well as responses to drugs within dynamical stress landscapes. Microfluidics have been proposed to bridge the gap between 2D cell culture studies and more complex in vivo animal studies that may not be able to support controllable quantitative studies[7,8,9].

An ideal in vitro system to characterize cancer cell dynamics should possess the ability to generate a heterogeneous microenvironment to mimic the adaptive cellular responses that may take place in a tumor, as well as allow for the observation of these dynamics at a single-cell resolution. In this article, we describe a microfluidic cell culture platform, a PDMS-based device called the "Evolution Accelerator" (EA), that allows for parallel in vitro studies of cancer cell dynamics at cellular resolution with real-time data acquisition over the course of weeks, while stably maintaining gradients of stress across the culture landscape. The design of this platform is based on our previous work, in which the evolutionary dynamics of organisms in a metapopulation can be accelerated[10,11]. Specifically, in a group of spatially separated populations that interact at some level, when exposed to a heterogeneous stress landscape, the most fit species can dominate in a local population faster compared with that of a large uniform population. The advantageous species then migrate to neighboring microhabitats in search of resources and space, and eventually dominate the entire population. As shown in **Figure 1**, the pattern of the microfluidic EA chip is composed of (i) a pair of serpentine channels that provide fresh media circulation and construct fixed boundary conditions for chemical diffusion, and (ii) the hexagonal cell culture region which consists 109 interconnected hexagonal and 24 half-hexagonal chambers in the center, resembling a honeycomb structure. The chip is 100 µm in depth. Media channels and cell culture region are connected with small slits (about 15 µm wide), which prevent direct media flow and the resulting shear stress across the cell culture area, yet still allow chemicals to diffuse through small slits and exchange nutrients, metabolic waste, etc. The generation of chemical gradients is demonstrated in **Figure 1B**, where one media channel contains 0.1 mM of fluorescein while the other channel is free of fluorescein. Cells are cultured on a gas permeable membrane, encapsulated by the microstructures through the positive back pressure on the membrane against the chip. The components of the device holder are illustrated in **Figure 2**, and

the experimental setup is illustrated in **Figure 3**, where the culture is maintained on an inverted microscope at 37 °C, with above 85% relative humidity, and conditioned under normoxia gas composition.

This system provides detailed observation of localized cellular interactions via brightfield and fluorescent channels and allows for spatially-resolved downstream assays such as immunofluorescence, Western blot, or mass spectrometry. We have previously demonstrated as a proof-of-principle of this microfluidic cancer-on-chip model on the long-term co-culture of epithelial and mesenchymal PC3 prostate cancer cells[12] as well as the emergence of drug-resistance polyploid giant cancer cells using the epithelial PC3 cell line[13]. While we present the application of this platform to understand the spatiotemporal dynamics of epithelial PC3 and mesenchymal prostate cancer cells under a stress gradient of docetaxel, the microfluidic system can be easily applied to any combination of cell lines and resource (i.e., drug, nutrient, oxygen) gradients.

Protocol

1. Fabrication of microfluidic device

1. Generate the desired microfluidic pattern using a layout design software (see **Supplemental Materials**).
2. Fabricate the photomask. See **Table of Materials** for more details.
    1. Utilizing a laser writer, write the pattern on a soda-lime glass plate coated with 100 nm of Cr and 500 nm of photoresist AZ1518.
    2. Develop the photoresist with developer AZ300MIF for 60 s.
    3. Etch away the chromium without protection from the photoresist using Cr-7 Chromium Etchant.
    4. Strip off residual photoresist using a photoresist stripper at 70 °C for 45 min.
3. Pattern the photoresist. See **Table of Materials** for more details.
    1. Spin coat HMDS on silicon wafer at 4000 rpm for 40 s.
    2. Spin coat photoresist AZ4330 on silicon wafer at 4000 rpm for 40 s.
    3. Soft bake the silicon wafer at 95 °C for 60 s.
    4. Utilize the mask aligner to expose UV to the silicon wafer.
    5. Develop the photoresist with developer AZ300MIF for 4 min.
4. Perform DRIE etching. See **Table of Materials** for more details.
    1. Dry-etch the wafer patterned with the photoresist using a Silicon Deep Reactive Ion Etching (DRIE) system for 100 µm depth.
    2. Strip off the photoresist with acetone and plasma etch with a plasma etcher.
5. Wafer oxidation and silanization. See **Table of Materials** for more details.
    1. Perform thermal oxidation on the etched silicon wafer in a furnace at 1100 °C for 1 h.
    2. Wait for the silicon wafer to cool down, and then place the wafer into a desiccator with a few drops of trichloro-1H,1H,2H,2H-perfluorooctyl-silane (PFOTS) dripped in a small container near the wafer.
    3. Pump the pressure of the desiccator to 0.5 atm at room temperature for 60 min. The silicon wafer mold should become hydrophobic after proper silanization, which can be tested by adding several droplets of water onto the wafer.
6. Soft lithography. See **Table of Materials** for more details.
    1. Mix pre-polymer and cross-linker (from polymethylsiloxane (PDMS) kit) at a 10:1 by weight ratio.
    2. Pour the mixed PDMS to create a 10 mm film in height onto the silanized silicon wafer mold.
    3. Degas the resulting PDMS-silicon wafer system in a desiccator for 30 min to 1 h.
    4. Incubate the PDMS-silicon wafer in a 70 °C incubator overnight to cure the PDMS.
    5. Once the PDMS is cured, peel the PDMS film off the silicon wafer carefully.
    6. Using biopsy needles, punch through-holes at the inlet ports based on the location of the pattern on the PDMS and employ a circular punch to cut chips 27 mm in diameter.
7. PDMS layer bonding.
    1. Heat cure two stacks of 27 mm PDMS cylinders (without patterning), which will become the reservoir layer and the capping layer of the device.
    2. Cut out two 7 mm circles around the inlets on the reservoir layer, and utilize a biopsy needle to punch through-holes at the inlet ports on the capping layer.
    3. Bond three stacks of PDMS (patterned stack, reservoir layer, capping layer) with oxygen plasma treatment.
    4. With the biopsy needle, punch through-holes at the outlets and the center port of the device.

2. Media and cell line preparation

1. Prepare media for culturing PC3 cell lines, including PC3-EMT and PC3-EPI: mix RPMI 1640 medium with 10% fetal bovine serum (FBS) and 1x antibiotic-antimycotic. Generate cell lines as described previously[14].
   NOTE: PC3 cell lines are maintained in the above media in humidified incubators at 37 °C with 5% CO_2. Split cells and subculture every 3 days, before they reach 100% confluency.
2. Transfect cell lines with cytoplasmic-labeled fluorescent markers for better visualization, as described previously[12], such that PC3-EMT expresses cytoplasmic GFP and PC3-EPI expresses cytoplasmic mCherry. Note that the technology is also compatible with any fluorescent-labeled cells as well as brightfield imaging of unlabeled cells.

3. Experimental setup

1. Fabrication of metal plate holder
    1. Fabricate a plate holder that is sufficient to hold simultaneous gas-permeable culture dishes for parallel experiments by machining or 3D printing. The 3D CAD file ("3-well plate.FCStd") can be found on GitHub as a reference (https://github.com/kechihl/3-well-plate).
    2. Unscrew the components of the holder (**Figure 2**) with a screwdriver. Disinfect the components via UV exposure for at least 1 h and leave in a sterile environment.
    NOTE: The holder is designed to provide substantial conditions for thermal equilibrium and ideal gas compositions, with gas channel inlets that allow for airflow. More details can be found in our previous work[12].
    3. Prepare up to three gas-permeable culture dishes, of which the cell culture membrane is relatively flexible.

2. Cell line seeding
    1. 24 hours before the start of the experiment, harvest PC3-EPI and PC3-EMT cells by trypsinization for 5 min. Add prewarmed culture media, then centrifuge at 150 x *g* for 3 min and discard the supernatant.
    2. Count cells of each PC3-EPI and PC3-EMT using a hemocytometer and isolate a total of 2.5 x 10^4 of each cell type for each gas-permeable culture dish.
    3. Mix and resuspend the two cell types in 2 mL of culture media and seed the cells into each of the gas-permeable culture dish.
    4. Leave the entire plate holder in the incubator overnight for cells to attach.
    5. Disinfect the PDMS devices via UV exposure for at least 1 h and leave in a sterile environment.

3. Setting up thermal control unit and gas supply system
    1. As shown in **Figure 3**, set up a gas supply system that consists of both CO_2 and O_2 control units, a gas pump, a gas mixing chamber, a humidifier or bubbler, and three separate sets of gas valves and pressure gauges. More details can be found in our previous work[12].
    2. Set up the CO_2 and O_2 control units such that they adjust the mixing rate of the gas from CO_2 and N_2 tanks and the O_2 source. Alternatively, any gas supply system that provides gas under normoxia condition would work.
    3. Make sure the gas that is combined in the mixing chamber and humidified by a bubbler such that the relative humidity is increased up to 85% (as read out from a relative humidity monitor) and that the gas leads to three independent gas valves with pressure gauges in order to control and monitor gas flow rate in the plate holder.
    4. Place the entire plate holder in an on-stage incubation thermal control unit with separate heating subunits for the lid and the bottom plate, with all units set at 37 °C. See **Table of Materials** for more details.

4. Installation of microfluidic device. See **Table of Materials** for more details.
    1. Identify that the detailed components of the 3-well plate holder are in order, as in **Figure 2**. Each of the three wells are identical and independent, with a pair of gas channels for each well. Every well possesses a gas-permeable culture dish holder, a PDMS chip holder, a glass window holder, and a pair of 35 mm glass windows. These components can be assembled using the fitted screws.
    NOTE: The glass windows ensure that there is a thermally-isolated space between the gas-permeable culture membrane and the well such that no water condensation occurs due to temperature differences at the interface. Note that the 3 wells are independent, and 3 experiments can be done separately.
    2. Pre-warm culture medium at 37 °C and degas in a vacuum chamber for 20 min.
    3. Treat the PDMS chips using an oxygen plasma system for 30 s in order to maintain hydrophilicity.
    4. Set up the syringe system. Load two syringes slowly with growth media and other two syringes with desired reagent of interest (media, media with drug, etc.). Connect each individual syringe to a 50 cm tubing (0.020" x 0.060"OD) by a 23 G dispensing needle into one hollow steel pin. Insert a hollow steel pin into the other end of the tubing.
    5. Prime the tubing and insert the steel pin into each PDMS chip through the capping layer. Fill up the reservoir layer and wet the PDMS pattern layer pattern with media. The reservoir layer works as an on-chip bubble trap to prevent air bubbles from getting into the microfluidic pattern.
    6. Load a 1 mL syringe with culture media. Connect the syringe to a 5 cm tubing (0.020" x 0.060"OD) by a 23 G dispensing needle into one hollow steel pin. Insert a hollow steel pin into the other end of the tubing and prime the tubing.
    7. Insert the hollow steel pin into the center hole of the chip, where excessive media can be extracted out from the chip later during the chip sealing process.
    8. As each PDMS device requires four 10 mL syringes loaded onto a syringe pump, load two 10 mL syringes per chip in the forward deck. Place the two other syringes in the withdraw deck of the syringe system.
    9. Place chip directly on top of the gas-permeable culture membranes (with cells already adhered to the membranes). In order to avoid entrapping microbubbles in the microfluidic pattern, dispense 1 mL of prewarmed and degassed media into the 35 mm gas-permeable culture dish before assembly, and then make sure that the chip approaches the liquid surface with a 15-degree tilt angle.
    10. Clamp the gas-permeable culture dish and the well in the gas-permeable culture dish holder for each chip, with the PDMS chip holder pushing the PDMS device downward.
    11. Tape a sheet of a sealer on top of the PDMS device and clamp with the PDMS chip holder in order to prevent the chip from drying out.
    12. Set media flow rate around the array to be 20 µL/h.
    13. Set the entire plate in the on-stage incubator on the motorized stage of an inverted microscope. Connect the gas supply system to the gas channels and pressurizing the gas-permeable culture membrane against the installed PDMS chip to ensure sealing of device. Maintain gauge pressure at 0.2 psi (1.4 x 10^4 Pa).
    14. Slowly extract excessive media in the chip using the 1-mL syringe from the center hole. Observe the chip under the microscope while extracting media and then stop extracting when the chip is sealed. Chip sealing should be obvious since a part of the cells would be crushed by the micro-structures.
    15. Connect the temperature sensing unit of the on-stage incubator to the 3-well plate and set to 37 °C.

4. Single-cell time-lapse imaging

1. Set up imaging software utilizing an inverted microscope to time-lapse image acquisition. Note that an inverted fluorescent microscope with fully motorized x-y stage, focus knob, shutter, and filter cubes is required for an EA experiment.
2. Configure software to acquire images across two channels at 10x magnification for each chip with automatic image-stitching after one round of autofocus. Be aware that automatic correction systems like Perfect Focus do not guarantee satisfying image quality. It is more recommended to generate a customized focus surface for long-term image acquisition based on either autofocus or manual focus across the chip.
3. Take images every hour and leave experiment running on the time scale of weeks. Monitor image quality on a daily basis and update the focus surface if necessary.
4. Prepare the PDMS chip and gas-permeable culture dish for subsequent immunofluorescent analysis, as described previously[13].

5. Image processing and analysis

1. Post-experimental processing
    1. Convert images into TIFF format for image processing and measurements utilizing Fiji/ImageJ.
    2. Compress TIFF files for ease of further image processing.

2. Fiji/ImageJ analysis
    1. To identify cells, perform Background Subtraction and Particle Analysis to identify fluorescent bright-spots for cell location detection and automatic cell counting.
    2. Utilize plugins (Manual Tracking, Chemotaxis, Migration Tool, Trackmate) to analyze cell motility and migration.

Representative Results

Validation of optimum cell growth on chip
A major goal of the experiment platform is to reproduce key components and interactions in a complex tumor microenvironment in a comprehensive manner, yet simple enough to provide quantitative, reliable and reproducible data. This goal can only be achieved if we have full control of the physical and biochemical environmental factors. We must either exclude the undesired factors or figure out a way to incorporate the uncontrollable factors into the quantitative model to correctly interpret the population behaviors.

The first test is to ensure optimum cell growth on the device. The cell proliferation rate on the device needs to be identical or comparable to their growth profile in conventional cell culture. As a proof of principle, human prostate cancer cell line PC3 cells were cultured in the PDMS chip without the presence of external stress. These cells were fluorescently-labeled in the cytoplasm so we could observe and quantify the population of cells using inverted fluorescent microscopy. Cells confluence, defined as the area that covered by cells, was measured at each microhabitat at different time frames given a selected intensity threshold on the fluorescent images using Fiji[15]. The growth curves of cells at each chosen position are plotted in **Figure 4**. The chosen positions are scattered across the chip, from the region near the apex of media inflow to the apex close to media outlets.

The growth curves in **Figure 4B** are well-aligned, suggesting the identicality of the cell proliferation profile as a function of position across the chip. The initial slope of the curves reveals the proliferation rate. The doubling time for cells in the device is around 24 hours as shown in **Figure 4B** from time 0 to 24 hours, which is the same as the doubling time in conventional cultureware[13]. Therefore, we conclude that without the presence of an external source of stress, the physical and biochemical factors are uniformly distributed, leading to the homogeneous and optimized cell growth from time 50 to 100 hours.

We further considered the ability to quantify cell dynamics between subpopulations in a microenvironment. GFP-expressing PC3-EMT and the mCherry-expressing PC3-EPI cell lines were co-cultured in the EA as shown in **Figure 5**. Cell confluence, defined as the percentage of area covered by the cells, is measured as the indication of the size of population. Starting from 40% confluence, the co-culture grew fully confluent within 3 days. Interestingly, we may observe the progression of each phenotype in the microenvironment. While the growth curve of total confluence is in the form of logistic growth model, the population of PC3-EMT continued to expand and PC3-EPI was suppressed in the asymptotic phase.

Demonstration of cell motility assay in a mixed population
Cell motility is an important phenotypic behavior. The motility distribution of a population can provide information about the physical interaction of cells, the mechanical properties of local microenvironment, and can sometimes be analyzed as an indication of epigenetic variation of cells. Given that our improved cell culture platform allows nearly continuous imaging, the advantage of having fine temporal resolution maximizes the potential of single cell tracking in a heterogeneous population.

We use the plugin TrackMate[16] in Fiji (http://fiji.sc) with customized macro to implement and automate the tracking process. TrackMate allows the user to implement and customize a tracking algorithm using a scripting language from the Fiji Script Editor. The tracking process is divided in a series of steps: the segmentation, filtering, and particle-linking processes.

As shown in **Figure 6B**, we performed a "wound healing assay" as a demonstration to study cell collective migration and cell-cell interaction. PC3-EPI and PC3-EMT cells were densely seeded in the center of the device and were allowed to freely migrate toward empty region. The normalized histogram of the speed of both phenotypes is plotted in **Figure 6C**. The velocity of PC3-EMT was significantly higher than PC3-EPI by a factor of 1.8x, which is consistent with the fact that the mesenchymal phenotype serves as a component of cutaneous wound healing with exceptional ability to migrate as opposed to the comparably stationary epithelial phenotype.

Further, in order to observe the progression of cell motility in a stress-free environment, we performed a long-term co-culture of PC3-EPI and PC3-EMT with uniform initial seeding density and tracked the distribution of cell velocity varying with time. As shown in **Figure 7A,B**, after 6 days of culture, as cells reached higher confluence, the distributions of cell speed for both phenotypes leaned toward the left tails.

We may compare the ratio of number of PC3-EPI to PC3-EMT in each class interval. As shown in **Figure 7C**, regardless of the days of culture or density of cells, PC3-EMT dominated the high-speed region while PC3-EPI occupied the low speed zone. Although the overall velocity decreased significantly for both phenotypes, PC3-EMT remained motile and was affected less by the crowdedness of the microenvironment as shown in **Figure 7D**. The average speed of PC3-EPI dropped around 40% while that of PC3-EMT only dropped 14%.

There are several factors that can affect the distribution of cell velocity and the average speed, such as the crowdedness of the population. Continuous cell tracking and monitoring over all subpopulation is essential to understand the progression of phenotypic behavior. For example, if we would like to quantify the level of the mesenchymal status of an unlabeled subpopulation, it would be more informative to acquire not only the distribution of the physical quantity (e.g., velocity) of the interested subpopulation as a function of time, but also that of all the rest of the coexisting subpopulation of cells.

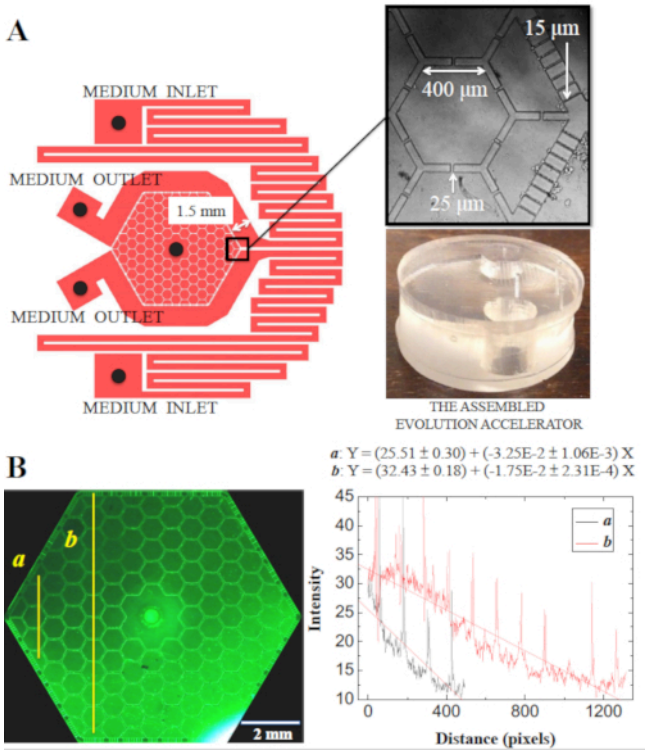

Figure 1: The syringe-pump-driven microfluidic EA chip. (**A**) The microfluidic device has two separate medium inlets, two outlets, and one central port for cell seeding or extraction of excessive medium. Note that between the medium inlets and the cell culture arrays, a pair of serpentine channels that allow the medium to equilibrate with the atmosphere passed below the gas-permeable membrane. (**B**) The generation of gradient. The syringes pump the medium with ~ 0.1 mM of fluorescein and no fluorescein respectively into the chip through the 2 medium inlets on the right, extracted out from the chip at the 2 medium outlets on the left. The concentration of fluorescein is proportional to the intensity of fluorescence signal, and is profiled near the medium inlets/outlets a and near the center b. Figure reproduced with permission from Lin et al. 2017[12]. Please click here to view a larger version of this figure.

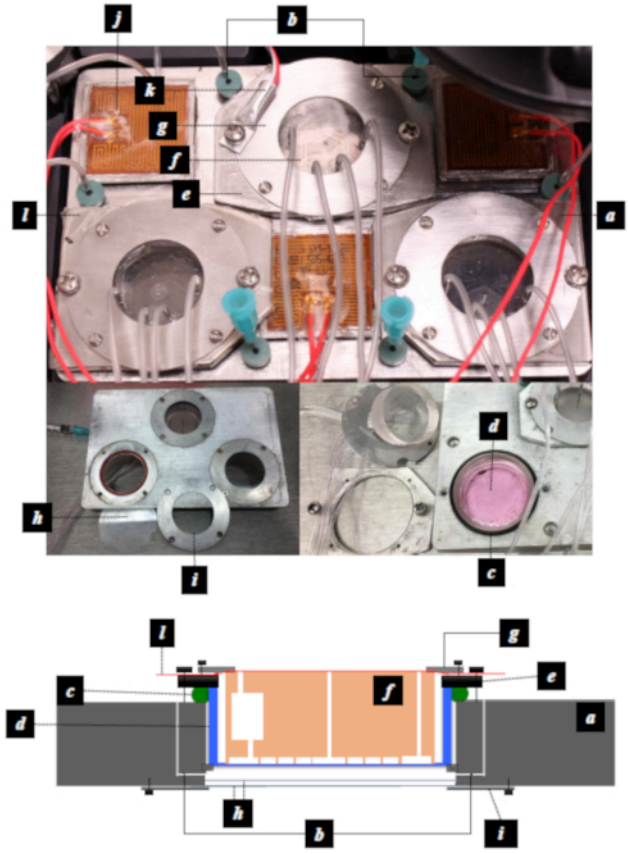

Figure 2: The components of the customized 3 well sample plate. (**a**) the main body of 3 well plate; (**b**) a pair of gas channels that allow conditioned atmosphere to be pumped in and vented out through the septa at the entrance of the gas channels; (**c**) an O-ring designed to seal the space between the well plate and the gas-permeable culture dish; (**d**) the 35 mm diameter gas-permeable culture dish; (**e**) the dish holder; (**f**) the PDMS device; (**g**) the PDMS chip holders; (**h**) the double layer 35 mm glass windows designed to maintain thermal isolation and prevent water condensation; (**i**) glass window holder; (**j**) heating pads; (**k**) temperature sensor; (**l**) the Adhesive sealer that keeps the chip from drying out. Figure reproduced with permission from Lin et al. 2017[12]. Please click here to view a larger version of this figure.

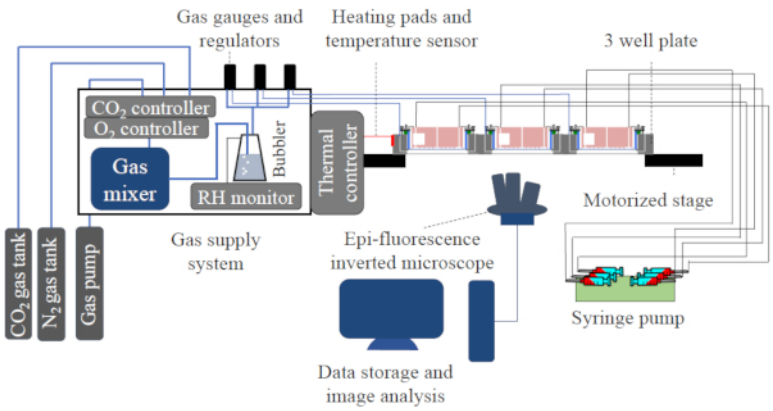

Figure 3: The schematic figure of the experimental setup. The setup of the experiment, including the gas supply system, gas channels connection, the medium supply connection and the imaging system. Figure reproduced with permission from Lin et al. 2017[12]. Please click here to view a larger version of this figure.

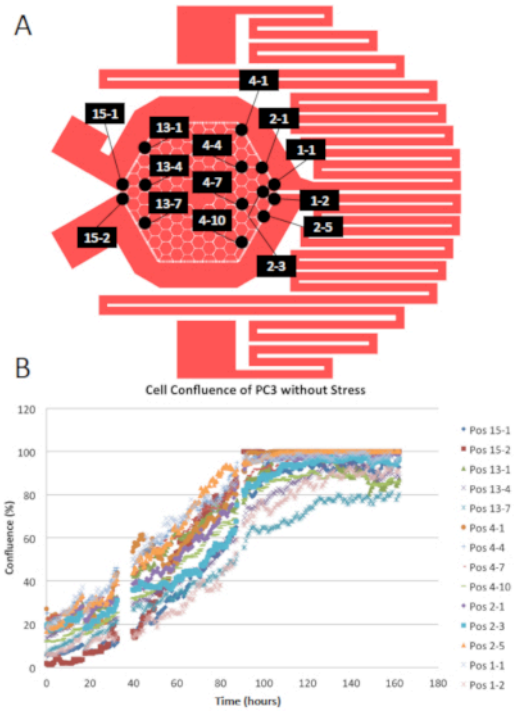

Figure 4: Growth curves of PC3 in the EA without stress. PC3 were cultured in EA without the presence of external stress. (**A**) Pattern of EA with position labels. (**B**) Growth curves of PC3 at the chosen positions in terms of cell confluence. Please click here to view a larger version of this figure.

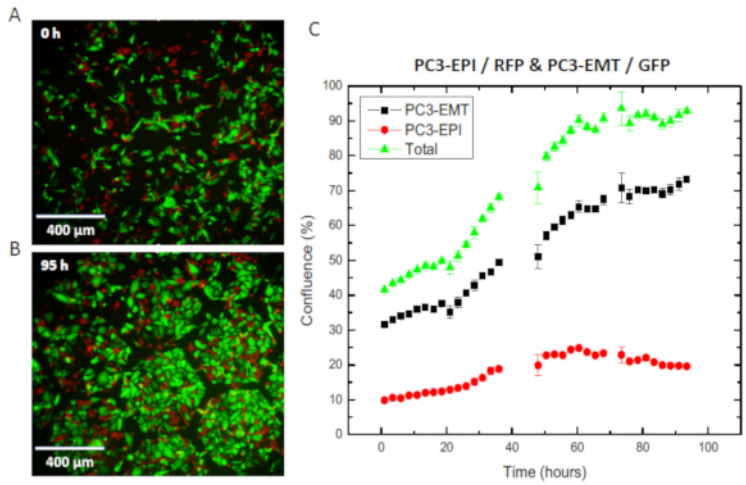

Figure 5: The co-culture of PC3-EPI and PC3-EMT in the EA without stress. PC3-EPI (red) and PC3-EMT (green) were co-cultured in the EA without the presence of external stress. (**A**) Overlay of two fluorescent channels at t = 0 h. (**B**) Fluorescent image taken at t = 95 h. (**C**) Growth curves in terms of cell confluence. Cell confluence of each cell type was measured on the entire chip. Each data point represents the average cell confluence at 3 consecutive time points taken at 15-min intervals. The error bars represent the standard deviation of cell confluence at the 3 consecutive time points. Please click here to view a larger version of this figure.

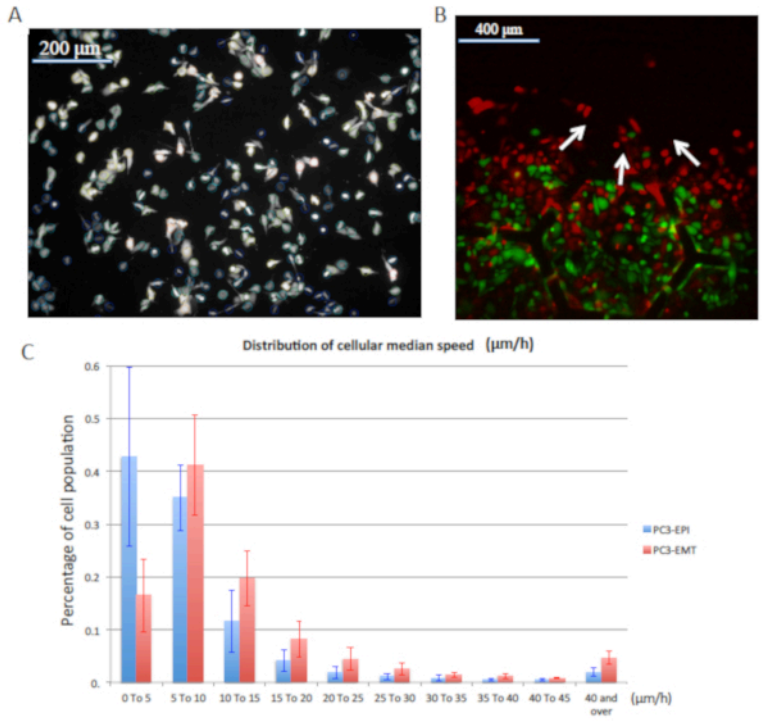

Figure 6: Cell motility assay in a mixed population. The demonstration of single cell tracking performance in a mixed population. (**A**) A demonstration of how cells are detected by Laplacian of Gaussian (LoG) segmentation. The circles indicate the location of cells detected by the LoG algorithm. The detected cells are linked from frame to frame based on the linear assignment problem to quantify cell motility. (**B**) The "wound healing assay" of PC3-EPI and PC3-EMT co-culture experiment. Cells were seeded locally up to 100% confluence with a clear boundary at the center. After the installation of the EA chip, cells were observed to migrate through the microhabitat array as indicated by the white arrows. (**C**) Normalized histogram of cell motility. PC3-EMT is faster than PC3-EPI by a factor of 1.8x. The error bars represent the standard deviation of 5 experiment samples. Please click here to view a larger version of this figure.

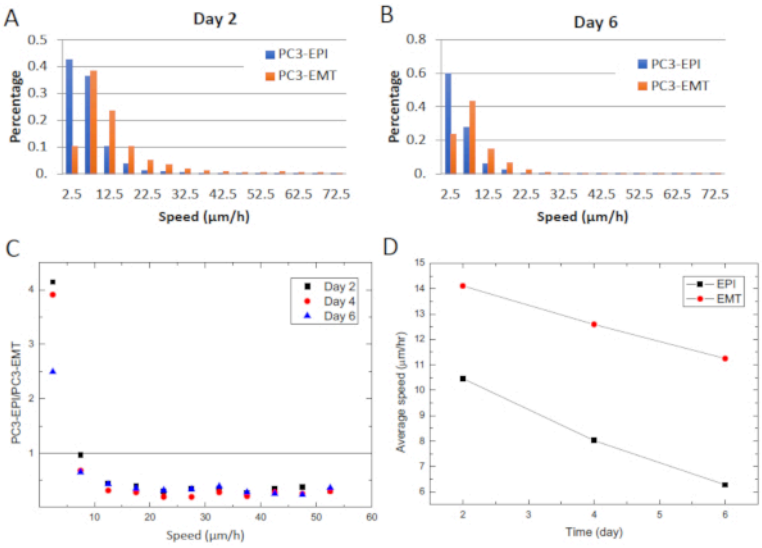

Figure 7: The motility assay of a long-term co-culture of PC3-EPI and PC3-EMT. A long-term co-culture of PC3-EPI and PC3-EMT with uniform initial seeding density. The distribution of cell velocity varies with time. (**A**) Normalized distribution of cell speed on day 2. (**B**) The normalized distribution of cell speed on day 6. (**C**) Ratio of number of PC3-EPI to PC3-EMT in each class interval. (**D**) Average speed of PC3-EPI and PC3-EMT as a function of time. Please click here to view a larger version of this figure.

Discussion

Conventional cell culture was developed almost a century ago and remains the most frequently used preclinical model in biomedical research, despite its proven limited ability to predict clinical results in cancer[17]. Animal models offer the highest physiological relevance and reasonable genetic similarity to humans, but have long been acknowledged to have significant limitations in predicting human outcomes[18]. Among all the existing preclinical models, microfluidic cancer-on-chip models appear to be the most promising candidate to satisfy the unmet need in cancer

research[9,19,20]. However, current cancer-on-chip models have yet to offer a platform that is able to reproduce key components and interactions to mimic a tumor microenvironment in a comprehensive manner, yet simple enough to provide reliable and reproducible quantitative data. Our representative data demonstrate that our microfluidic cell culture technology provides stable physical and biochemical conditions for long-term cell culture in heterogeneous microenvironments. This multifunctional platform allows the sophisticated adjustment of a time--dependent chemical gradient as well as ambient gas composition. The platform is portable and compatible to most of the fluorescent inverted microscopes for high--resolution real-time imaging, which offers multidimensional information of cells as a function of time, including cell morphology, population dynamics, cell motility and cell migration on a single-cell level.

Compared to our previous work[11], we note that this pressure-sealing packaging and assembly method for our microfluidic device enables numerous downstream experiment capacities (e.g., FACS, local metabolite extraction, sub-clonal populations expansion, IF, DNA/RNA FISH, etc.) complementary to the time-lapse images taken in the course of the experiments. This capability of removing cells from specific locations in a heterogenous culture is a major advance compared to earlier devices, where the sealing surface to a chip had to be removed before one could access the culture[11]. Further, even in that case, the act of removing the cover significantly disturbed the culture so that local testing of cells on a single to few habitat levels was not possible. Such localized extraction was possible in our case due to the soft "resealable" nature of the flexible gas-permeable membrane.

There are several critical steps in the presented protocol. First of all, to initiate a long-term experiment with stable fluidic dynamics, microbubbles need to be avoided as much as possible. Therefore, it is important to prewarm and degas the culture medium (step 3.4.2) before loading the media into the syringes. The manipulation of media loading and dispensing should be done slowly and gently to prevent bubble formation. The PDMS pattern should be treated with oxygen plasma (step 3.4.3) before connecting to the culture media supply system. Oxygen plasma treatment ensures the hydrophilicity of the PDMS surface and significantly reduces the possibility of microbubble entrapping. In step 3.4.7., when placing the chip on top of the cell culture membrane, the PDMS chip should approach the liquid surface with a 15-degree tilt angle to get rid of the bubbles (if any) on the liquid surface inside the culture dish. Secondly, the pressure-sealing method requires a stable gas supply system that pressurizes the cell culture membrane. The pressure should be set between 0.2 to 0.6 psi. Pressure lower than 0.2 psi is insufficient for chip sealing. Above 1.2 psi, a significant amount of gas would permeate through the membrane and generate bubbles within the microfluidic pattern. We note that if the components of the metal 3-well plate are not properly assembled (including the plate body, the gas-permeable culture dish holder, a PDMS chip holder, a glass window holder, O-rings, and a pair of 35 mm glass windows), one would identify gas leakage as the pressure reading would be irresponsive to the increase of the gas flow. The leakage issue can be resolved simply by doing a leakage test and then reassembling the components.

The major form of data acquired with the utilization of the EA technology is through imaging. As mentioned previously, the EA technology can be installed on any inverted microscope. However, to fully exploit the advantages of the system, it is highly recommended to install the system on an inverted fluorescent microscope equipped with fully motorized x-y stage, motorized focus knob, motorized shutter, and motorized filter cube. Also, be aware that Perfect Focus might not guarantee satisfying image quality. We suggest using an imaging software that allows multi-dimensional image acquisition and customized imaging script. Keeping the images well-focused could be challenging without a periodic (every 24 hours or 48 hours) autofocus command, which generated a customized focus surface during the image acquisition cycle.

The presented microfluidic EA technology has been implemented to study the adaptation and evolution dynamics in prostate cancer cell metapopulations under a chemotherapeutic stress landscape[12]. We have also demonstrated the emergence of drug-resistance polyploid giant cancer cells in this tumor-like heterogeneous micro-ecology, showing that environmental heterogeneity combined with cell migration within tumor population would cause amplification on the emergence of resistant phenotypes[13]. With the ability to control and monitor the behaviors of mixed tumor cell populations under well-controlled stress gradients, our microfluidic EA technology may also serve as a platform to study regulatory mechanisms and the phenotypic transformation involved in EMT in the context of cancer therapeutic strategies[21]. Last but not least, the presented pressure-sealing packaging method can also be implemented in other microfluidic systems that require the sophisticated adjustment of ambient gas composition as well as the downstream experiment capacities. For instance, the same packaging method was used to incorporate different microfluidic pattern to study how bacterial population waves propagate through physical barriers[22].

In summary, collective population dynamics are qualitatively different from single-cell behaviors. The microfluidic EA technology allows the quantitative study of the evolutionary dynamics and phenotypic behaviors individually and collectively as a function of time. This technology may present a more physiologically relevant in vitro model for cancer research, and potentially for preclinical drug development and screening.

Disclosures

No conflicts of interest declared.

Acknowledgments

This work was supported by NSF PHY-1659940.

References

1. Meacham, C. E., Morrison, S. J. Tumour heterogeneity and cancer cell plasticity. *Nature.* **501** (7467), 328-337 (2013).
2. Whiteside, T. L. The tumor microenvironment and its role in promoting tumor growth. *Oncogene.* **27** (45), 5904-5912 (2008).
3. Lambert, G. et al. An analogy between the evolution of drug resistance in bacterial communities and malignant tissues. *Nature Reviews Cancer.* **11** (5), 375-382 (2011).
4. Tannock, I. F., Lee, C. M., Tunggal, J. K., Cowan, D. S., Egorin, M. J. Limited penetration of anticancer drugs through tumor tissue: a potential cause of resistance of solid tumors to chemotherapy. *Clinical Cancer Research.* **8** (3), 878-884 (2002).

5. Grantab, R.H., Tannock, I.F. Penetration of anticancer drugs through tumour tissue as a function of cellular packing density and interstitial fluid pressure and its modification by bortezomib. *BMC Cancer.* **12**, 214 (2012).
6. Fu, F., Nowak, M.A., Bonhoeffer, S. Spatial Heterogeneity in Drug Concentrations Can Facilitate the Emergence of Resistance to Cancer Therapy. *PLoS Computational Biology.* **11** (3), e1004142 (2015).
7. Bogorad, M. I. et al. In vitro microvessel models. *Lab on a Chip.* **15** (22), 4242-4255 (2015).
8. Caballero, D. et al. Organ-on-chip models of cancer metastasis for future personalized medicine: From chip to the patient. *Biomaterials.* **149**, 98-115 (2017).
9. Caballero, D., Blackburn, S. M., De Pablo, M., Samitier, J., Albertazzi, L. Tumour-vessel-on-a-chip models for drug delivery. *Lab on a Chip.* **17** (22), 3760-3771 (2017).
10. Zhang, Q. et al. Acceleration of emergence of bacterial antibiotic resistance in connected microenvironments. *Science.* **333** (6050), 1764-7 (2011).
11. Wu, A. et al. Ancient hot and cold genes and chemotherapy resistance emergence *Proceeding of the National Academy of Sciences of the United States of America.* **112** (33), 10467-72 (2015).
12. Lin, K. C. et al. Epithelial and mesenchymal prostate cancer cell population dynamics on a complex drug landscape. *Convergent Science Physical Oncology.* **3** (4), 045001 (2017).
13. Lin, K. C. et al. The role of heterogeneous environment and docetaxel gradient in the emergence of polyploid, mesenchymal and resistant prostate cancer cells. *Clinical & Experimental Metastasis.* **36** (2), 97-108 (2019).
14. Roca, H. et al. Transcription factors OVOL1 and OVOL2 induce the mesenchymal to epithelial transition in human cancer. *PloS One.* **8** (10), e76773 (2013).
15. Schindelin, J. et al. Fiji: an open-source platform for biological-image analysis. *Nature Methods.* **9** (7), 676-682 (2012).
16. Tinevez, J.-Y. et al. Trackmate: An open and extensible platform for single-particle tracking. *Methods.* **115**, 80-90 (2017).
17. Caballero, D. et al. Organ-on-chip models of cancer metastasis for future personalized medicine: From chip to the patient. *Biomaterials.*, **149**, 98-115 (2017).
18. Akhtar, A. The flaws and human harms of animal experimentation. *Cambridge Quarterly of Healthcare Ethics.*, **24** (4), 407-419 (2015).
19. Sontheimer-Phelps, A., Hassell, B.A., Ingber, D.E. Modelling cancer in microfluidic human organs-on-chips. *Nature Reviews Cancer.*, **19** (2) 65-81 (2019).
20. Bogorad, M.I., DeStefano, J., Karlsson, J., Wong, A.D., Gerecht, S., and Searson, P.C. Review: in vitro microvessel models. *Lab on a Chip.*, **15**, 4242-4255 (2015).
21. Zañudo, J.G.T. et al. Towards control of cellular decision-making networks in the epithelial-to-mesenchymal transition. *Physical Biology.* **16** (3), 031002 (2019).
22. Morris, R.J. et al. Bacterial population solitary waves can defeat rings of funnels, *New Journal of Physics.* **19** (3), 035002 (2017).

